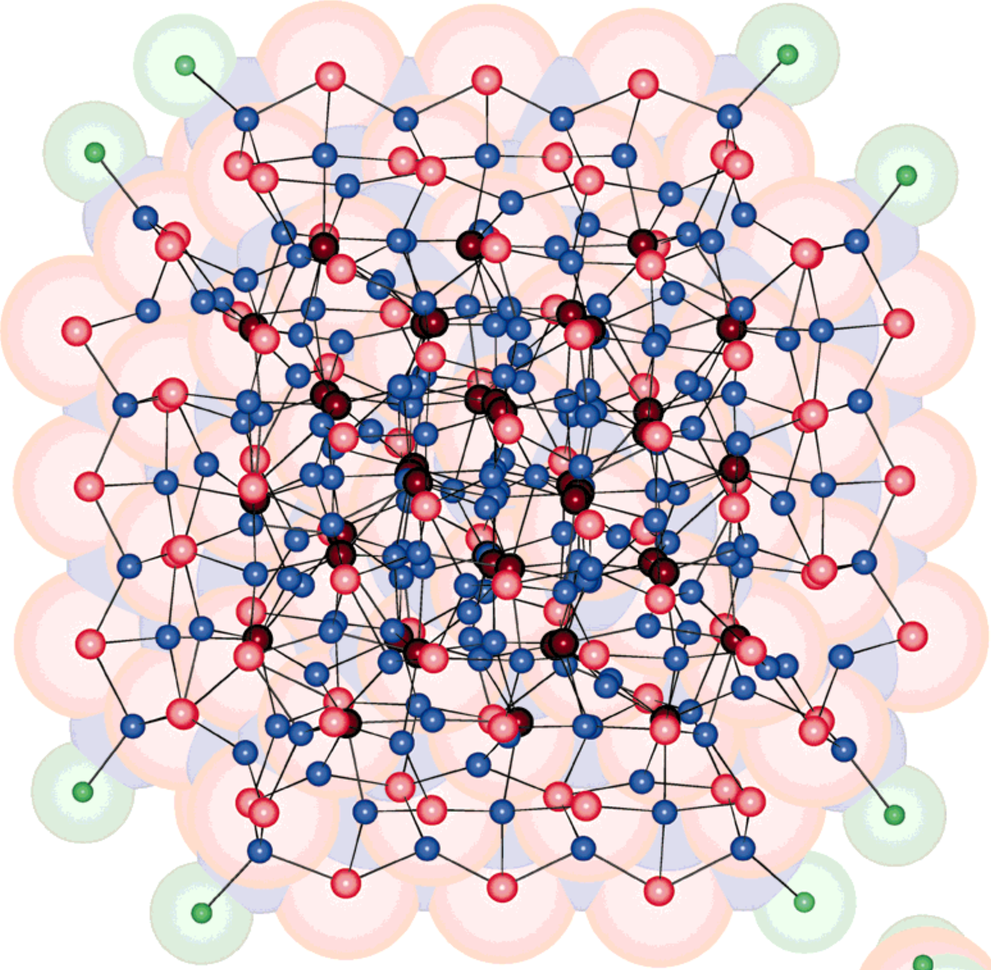

A distorted cube-like cluster with edges of about 2.3 nm in length are formed by the Ag atoms (blue), Se^{2-} ligands (dark red), and Se atoms (light red) of the Se*n*Bu groups in $[Ag_{172}Se_{40}(SenBu)_{92}(dppp)_4]$ (dppp = bis(diphenylphosphanyl)propane).

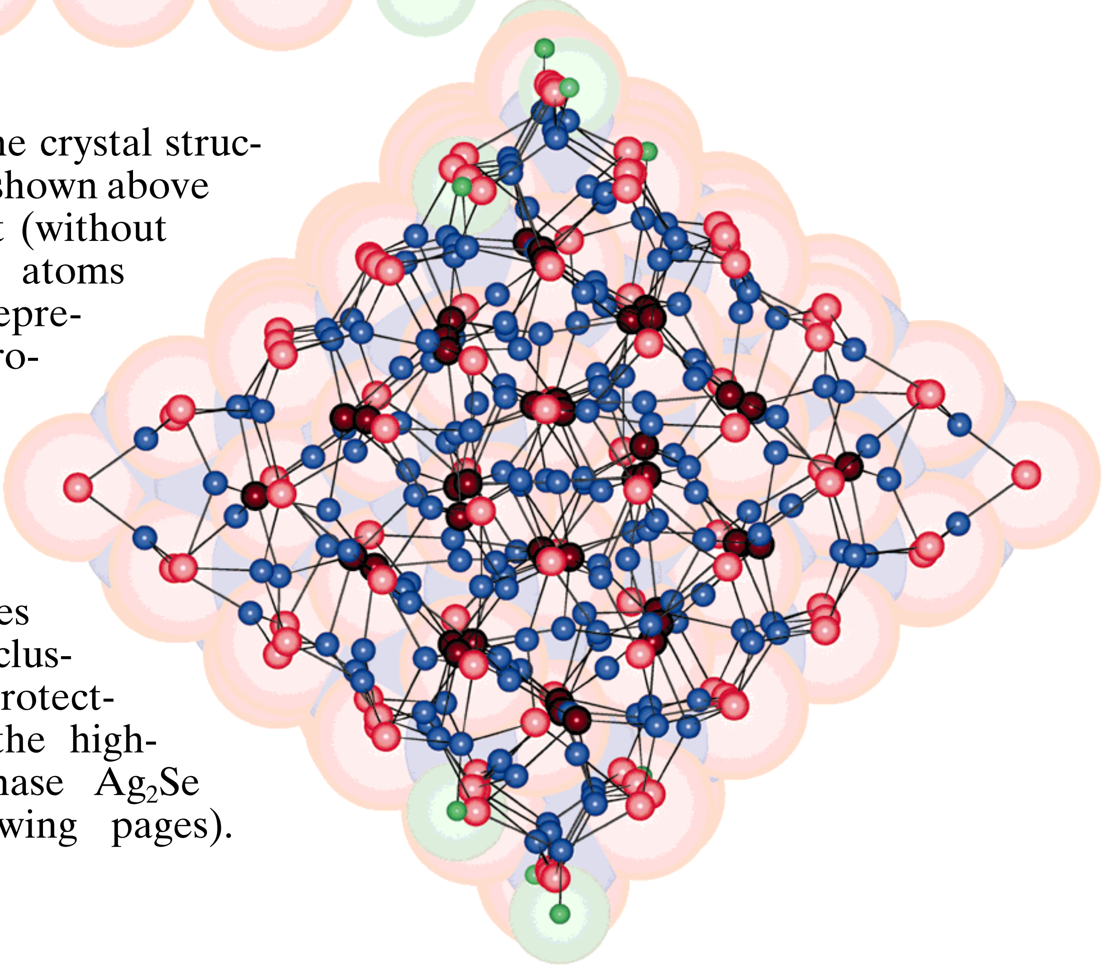

The result of the crystal structure analyses is shown above and to the right (without C atoms, P atoms green); the representations are rotated by 90° with respect to each other. The topology of the Se atoms indicates that the Ag–Se cluster is a ligand-protected section of the high-temperature phase Ag_2Se (see the following pages).

1433-7851/98/3719-2639 $ 17.50+.50/0

Synthesis and Structure of New Ag–Se Clusters: $[Ag_{30}Se_8(SetBu)_{14}(PnPr_3)_8]$, $[Ag_{90}Se_{38}(SetBu)_{14}(PEt_3)_{22}]$, $[Ag_{114}Se_{34}(SenBu)_{46}(PtBu_3)_{14}]$, $[Ag_{112}Se_{32}(SenBu)_{48}(PtBu_3)_{12}]$, and $[Ag_{172}Se_{40}(SenBu)_{92}(dppp)_4]$**

Dieter Fenske,* Nianyong Zhu, and Timo Langetepe

Dedicated to Professor Hans Bock
on the occasion of his 70th birthday

The synthesis, structure, and physical properties of large metal clusters are being investigated in many research groups.[1] A part of this interest lies in the metal chalcogenide clusters. Although a remarkably large number of transition metal sulfur clusters have been reported, there are significantly fewer selenium and tellurium analogues known, or even clusters with selenato and tellurato ligands.[2, 3] In the last few years interest in this class of compounds has increased dramatically, in that one can use them, for example, as precursors in the production of semiconducting metal selenides and tellurides. In the meantime a considerable number of multinuclear metal selenide cluster complexes are known which are protected by a ligand shell from further reaction to stable binary selenides. Examples for this are $[Ni_{34}Se_{22}(PPh_3)_{10}]$, $[Cu_{70}Se_{35}(PEt_3)_{22}]$, and $[Cu_{146}Se_{72}(PPh_3)_{30}]$.[4–6] These compounds are formed from the reaction of PR_3 complexes (R = organic group) with metal halides and $Se(SiMe_3)_2$. Very often though the thermodynamically stable metal selenides are formed. Calculations have shown that the PR_3-stabilized cluster complexes are metastable.[7, 8] With the above method it is possible, for example, to obtain copper chalcogenide clusters which can be described as a section of the structure of the binary Cu_2E phase (E = S, Se, Te) surrounded by PR_3 ligands.

In contrast, the synthesis of analogous silver clusters is considerably more difficult. The reaction of AgCl with, for example, $Se(SiMe_3)_2$ in the presence of PR_3 normally affords insoluble Ag_2Se. On the other hand, the reaction of AgCl, PR_3, and $RTeSiMe_3$ preferably provides silver clusters with Te^{2-} and TeR^- ligands. The structure of the cluster complexes formed depends very much upon the tertiary phosphane used and also on the organic group bound to tellurium. Some examples of compounds with known structures are:[9] $[Ag_6(TenBu)_6(PEt_3)_4]$, $[Ag_{10}(TePh)_{10}(PMe_3)_2]_\infty$, $[Ag_{30}(TePh)_{12}Te_9(PEt_3)_{12}]$, $[Ag_{32}(TenBu)_{18}Te_7(PEt_3)_6]$, $[Ag_{46}(TeMes)_{12}Te_{17}(PEt_3)_{16}]$, and $[Ag_{48}(TenBu)_{24}Te_{12}(PEt_3)_{14}]$. We report herein on further Ag clusters which can be isolated from the reaction of silver carboxylates with $RSeSiMe_3$ and PR_3 or bidentate phosphanes.

The reaction of $PnPr_3$, $tBuSeSiMe_3$, and silver benzoate in pentane at −40°C affords $[Ag_{30}Se_8(SetBu)_{14}(PnPR_3)_8]$ (**1**) in the form of light-senstitive orange crystals [Eq. (1)]. At

$$PhCO_2Ag \xrightarrow[PnPr_3]{tBuSeSiMe_3} [Ag_{30}Se_8(SetBu)_{14}(PnPr_3)_8] \quad \mathbf{1} \qquad (1)$$

higher temperatures only Ag_2Se can be isolated. Compound **1** crystallizes in the space group $P\bar{1}$ and possesses an inversion center. The structure of **1** is shown in Figure 1 and consists of

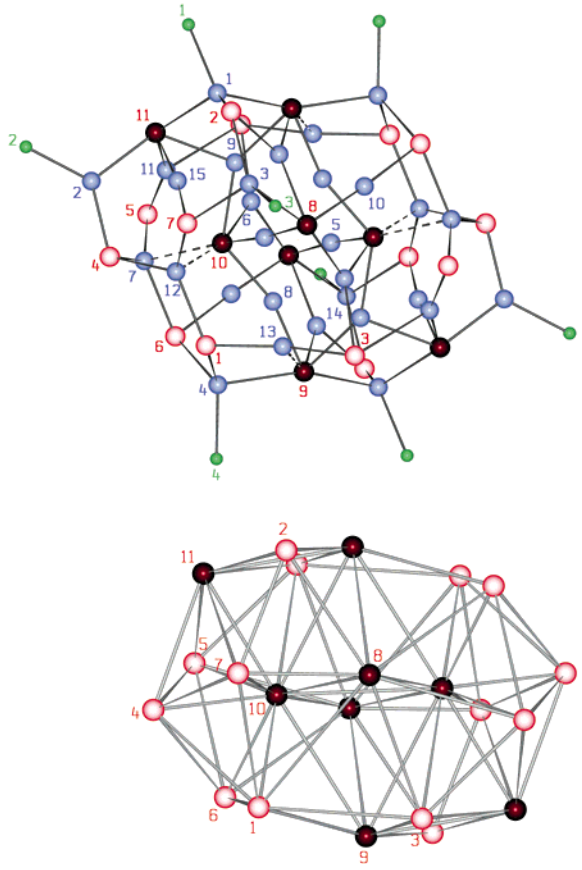

Figure 1. Top: molecular structure of **1** (without C atoms).[12] The P and Ag atoms are depicted in green and blue, respectively, Se^{2-} ligands are dark red, and Se atoms from the SetBu ligands are light red. For the sake of clarity only the atom number is given and the corresponding atom type can be deduced from the color. Bottom: Se atom skeleton. Selected bond lengths (±0.2 pm) and angles (±0.1°): Ag1–P1 247.3, Ag1–Se2 270.5, Ag1–Se9 285.5, Ag1–Se11 288.5, Ag5–Se8 251.5, Ag5–Se10 250.7, Ag7–Se4 260.6, Ag7–Se5 258.2, Ag7–Se6 269.4, Ag7–Se10 299.9, Ag9–Se9 261.8, Ag9–Se10 270.3, Ag9–Se11 280.5; Se8-Ag5-Se10 174.8, Se9-Ag9-Se10 143.1, Se9-Ag9-Se11 113.6, Se10-Ag9-Se11 102.3.

an $Ag_{30}Se_{22}$ cluster, in which the Ag atoms are coordinated in different ways and the Se atoms exist as Se^{2-} ligands and $SetBu^-$ groups. The Se^{2-} ligands are bound in different ways: the atoms Se8 – Se10 act as μ_6-bridging ligands, whereas Se11 is μ_5-bridging ligand. They exhibit both short (249.8 – 270.2(2) pm) and long (276.2 – 305.0(2) pm) bond lengths to the silver atoms. The selenium atoms of the SetBu groups act as μ_2- and μ_3-bridging ligands (μ_2-Se: Se3, Se5; Ag–Se: 252.1 – 262.0 pm; μ_3-Se: Se1, Se2, Se4, Se6, Se7; Ag–Se: 251.5 – 276.4(2) pm).

Ten silver atoms (Ag5, Ag8, Ag10, Ag11, Ag15, and their symmetry equivalents) are almost linearly coordinated by two Se atoms (Se-Ag-Se: 157.2 – 176.7°). These Ag atoms are bound to both Se^{2-} and $SetBu^-$ ligands (Ag–Se: 249.8 – 255.9(2) pm). The eight Ag atoms bound to the P atoms of

---

[*] Prof. Dr. D. Fenske, Dr. N. Zhu, T. Langetepe
Institut für Anorganische Chemie der Universität
Engesserstrasse, Geb. 30.45, D-76128 Karlsruhe (Germany)
Fax: (+49) 721-661921

[**] This work was supported by the Deutsche Forschungsgemeinschaft (SFB 195).

the phosphane ligands (Ag1 – Ag4 and symmetry equivalents) have different coordination modes. Atom Ag2 has a distorted trigonal-planar environment, coordinated by P2, an Se*t*Bu^{-}, and an Se^{2-} ligand. In contrast, Ag1 is bound to one Se*t*Bu^{-} (Se2) and two Se^{2-} (Se9, Se11) ligands, and to P1 in a distorted tetrahedral environment. Atoms Ag3 and Ag4 have likewise distorted tetrahedral coordination, but are each bound to a P atom from a P*n*Pr group, one Se^{2-}, and two Se*t*Bu^{-} ligands. Of the other twelve silver atoms, eight have distorted trigonal coordination (Ag6, Ag9, Ag13, Ag14) and Ag7 and Ag12 are bound to Se*t*Bu^{-} and Se^{2-} ligands in distorted tetrahedral environment. Figure 1 (bottom) shows that the Se atoms form a layered structure in which the first and third layers contain six Se atoms. The remaining ten Se atoms form the middle layer. Within the Se polyhedron, all the Se–Se distances are larger than 386 pm.

The reaction of silver benzoate, PEt$_3$, and *t*BuSeSiMe$_3$ in THF affords cluster **2** in a yield of 60 % [Eq. (2)]. The reaction temperature must not exceed −20 °C, otherwise only an

$$\mathrm{PhCO_2Ag} \xrightarrow[\mathrm{PEt_3}]{t\mathrm{BuSeSiMe_3}} [\mathrm{Ag_{90}Se_{38}(Se}t\mathrm{Bu)_{14}(PEt_3)_{22}}] \quad \mathbf{2} \qquad (2)$$

amorphous product is isolated along with Ag$_2$Se. Cluster **2** possesses an inversion center and crystallizes in the form of black platelets in the space group $P\bar{1}$. The structure of **2** is shown in Figure 2. The organic groups bound to phosphorus and selenium are omitted for the sake of clarity. Compound **2** contains 90 Ag and 38 Se^{2-} centers, as well as 14 Se*t*Bu^{-} and 22 PEt$_3$ ligands. The Se atoms form a torus-shaped polyhedron, which is made up of Se$_3$ faces (Figure 3); however, there are no bonding interactions between the Se atoms. The light red Se atoms of the Se*t*Bu^{-} groups are found at the surface of the polyhedron, which has approximately D_{6h} symmetry. Atoms Se7 and Se26 are found on the sixfold axis. The remaining Se atoms form two shells: the first inner sphere contains only Se^{2-} centers, while the second outer sphere contains both Se^{2-} and Se^{-} centers from the Se*t*Bu groups. The Se atoms of the 14 Se*t*Bu groups act as μ_2 (Se5, Ag–Se5: 250.4 – 252(2) pm) and μ_3 bridges (Se1 – Se4, Se6, Se7; Ag–Se: 251.5 – 297.8(2) pm). The Se^{2-} atoms also have different coordination modes. The Se^{2-} atoms in the outer shell act either as μ_4 or μ_5 bridges (Se10 – Se13, Se15 – Se17, Se21, Se24; Ag–Se: 250.2 – 305.6(2) pm). In contrast, the remaining Se^{2-} centers each form five to eight bonds to silver atoms.

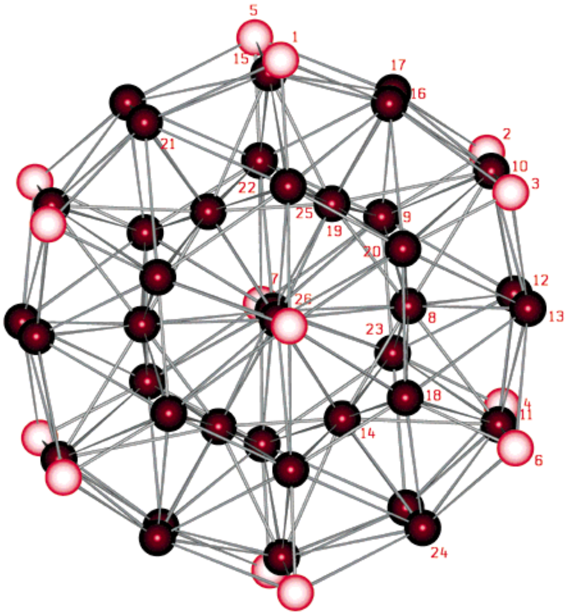

Figure 3. Part of the Se skeleton in **2**. The Se^{2-} atoms are shown in dark red, and Se atoms from the Se*t*Bu ligands in light red.

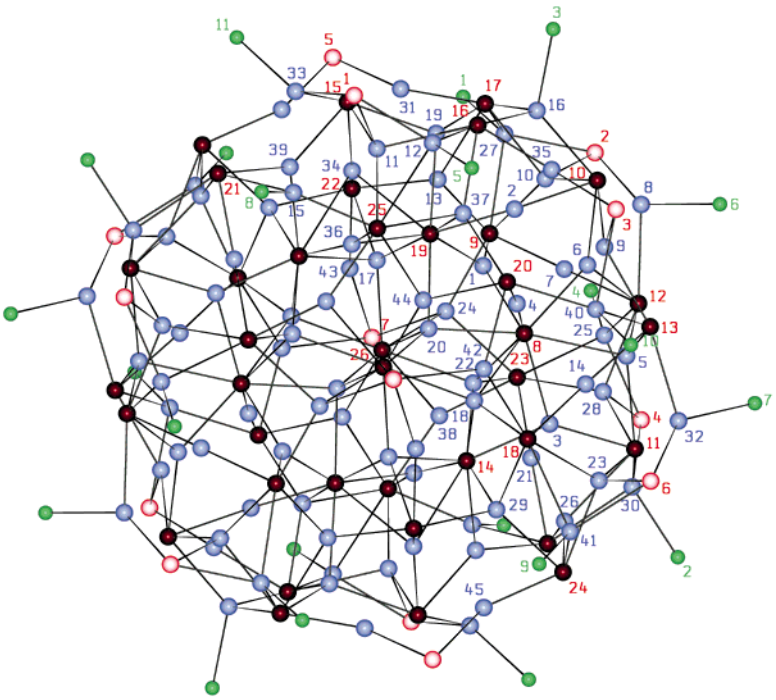

Figure 2. Molecular structure of **2** (without C atoms).[12] The P atoms are colored green, Se atoms from the Se*t*Bu ligands light red, Se^{2-} ligands dark red, and the Ag atoms blue. The atom number is given and the corresponding atom type can be deduced from the color. Selected bond lengths (±0.4 pm) and angles (±0.1°): Ag7–Se9 249.3, Ag7–Se12 250.2, Ag1–Se8 271.7, Ag1–Se9 261.9, Ag1–Se19 280.1, Ag19–Se15 274.8, Ag19–Se16 276.9, Ag19–Se17 272.2, Ag19–Se19 292.5; Se9-Ag7-Se12 176.7, Se8-Ag1-Se19 94.0, Se8-Ag1-Se9 136.4, Se9-Ag1-Se19 129.5, Se15-Ag19-Se16 106.1, Se15-Ag19-Se17 118.3, Se15-Ag19-Se19 106.3, Se16-Ag19-Se17 117.1, Se17-Ag19-Se19 108.2, Se16-Ag19-Se19 98.8.

A description of the coordination relationships is difficult as the Ag–Se bond lengths vary over a large range. For the Ag atoms one can recognize different distorted coordination polyhedra. The Ag atoms that are bound to PEt$_3$ groups are coordinated either in trigonal-planar (Ag8, Ag15, Ag32, Ag33) or in distorted tetrahedral fashion (Ag12, Ag16, Ag25, Ag27, Ag30, Ag40, Ag41) to the Se atoms of the Se*t*Bu groups, the remaining 68 Ag atoms are bound only to Se^{2-} centers. Of the 68 Ag atoms, 20 are bound in a distorted linear fashion to two Se^{2-} neighbors (Ag2, Ag4, Ag7, Ag9, Ag14, Ag21, Ag31, Ag35, Ag38, Ag43, Ag45; Ag–Se 249.3 – 259.1(4) pm; Se-Ag-Se: 147.5 – 176.7(3)°). A further 28 Ag atoms have distorted trigonal-planar environments (Ag1, Ag3, Ag6, Ag10, Ag13, Ag17, Ag23, Ag26, Ag34, Ag36, Ag39, Ag42, Ag44, Ag–Se: 255.9–293.2(4) pm). The remaining 20 silver atoms are bound to Se^{2-} atoms in a distorted tetrahedral manner (Ag5, Ag11, Ag18, Ag19, Ag20, Ag22, Ag24, Ag28, Ag29, Ag37; Ag–Se: 258.6–305.6(49) pm).

The reaction of silver laurate, P*t*Bu$_3$, and *n*BuSeSiMe$_3$ leads to the formation of $[Ag_{114}Se_{34}(SenBu)_{46}(PtBu_3)_{14}]$ (**3**; Figure 4). If the monodentate phosphane ligand is replaced by bis(diphenylphosphanyl)propane (dppp) under the same reaction conditions (−30 °C), the largest Ag cluster known up till now is formed, $[Ag_{172}Se_{40}(SenBu)_{92}(dppp)_4]$ (**4**) [Eq. (3)].

$$\begin{array}{ll} [Ag_{114}Se_{34}(SenBu)_{46}(PtBu_3)_{14}] & \mathbf{3} \\ \quad\uparrow PtBu_3 & \\ C_{11}H_{23}CO_2Ag + nBuSeSiMe_3 & \qquad (3) \\ \quad\downarrow dppp & \\ [Ag_{172}Se_{40}(SenBu)_{92}(dppp)_4] & \mathbf{4} \end{array}$$

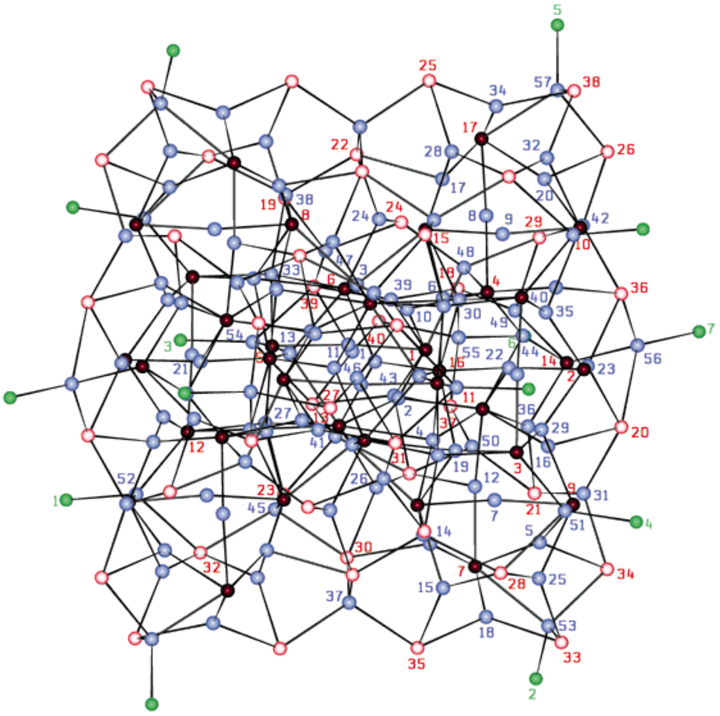

Figure 4. Molecular structure of **3**.[12] For the sake of clarity the atoms of the P*t*Bu$_3$ and Se*n*Bu ligands are not shown. (P atoms are green, Ag atoms blue, Se^{2-} ligands dark red, and the Se atoms of the Se*n*Bu light red.) The atom number is given and the corresponding atom type can be deduced from the color. Selected bond lengths (±0.4 pm) and angles (±0.1°): Ag11–Se1 250.3, Ag11–Se5 247.2; Ag1–Se6 272.3, Ag1–Se13 269.4, Ag1–Se16 262.6; Ag3–Se6 262.9, Ag3–Se8 285.5, Ag3–Se13 264.1, Ag3–Se15 282.8, Se1-Ag11-Se5 175.1; Se6-Ag1-Se13 108.9, Se6-Ag1-Se16 127.3, Se13-Ag1-Se16 122.6, Se6-Ag3-Se8 86.2, Se6-Ag3-Se13 163.9, Se6-Ag3-Se15 103.1, Se8-Ag3-Se13 105.4, Se8-Ag3-Se15 98.3, Se13-Ag3-Se15 86.6.

Clusters **1** and **2** are spherical and show no similarity to the bulk material structures of Ag_2Se and Ag_2S.[10] In contrast there is a remarkable agreement with respect to the topology of the Se centers between clusters **3** and **4**, and Ag_2E (E = S, Se). The selenium skeletons of **3** and **4** (Figure 5) correspond to a distorted cubic-centered structure that is also found in Ag_2Se. Therefore, the cluster structures of **3** and **4** can be described as different sizes of cross sections of Ag_2Se.

We have already observed similar size-dependent structural changes in the PR_3-stabilized Cu_2E clusters (E = S, Se),[4–6, 11] though the transition to cross sections from the structure of the binary Cu_2E phase already occurs with 70 Cu atoms. It is not surprising that the dependence of the structures of ionic clusters in the gas phase is likewise controlled by the number of ions. Examples for this are $(MgCl_2)_n$, $(KCl)_n$, and $(LiF)_n$[13] as well as Cu_2E clusters in the gas phase.[14]

As already described in the structures of **1** and **2**, the Se^{2-} and Se*n*Bu$^-$ ligands act as bridges between the Ag atoms in both **3** (Figure 4) and **4** (Figure 6). The Se*n*Bu groups act as either μ_3- or μ_4-bridging ligands (**3**: Ag–Se: 249.8–306.4(3) pm; **4**: Ag–Se: 241.3–306.5(3) pm). The Se^{2-} centers in **3** function as μ_4-, μ_5-, μ_6-, and μ_7-bridging ligands, and the Ag–Se distances lie in the range of 247–309 pm. In **4** the coordination relationships are significantly more complex. Within Ag–Se distances of 244–303 pm the Se^{2-} centers act as μ_5, μ_6, μ_7, and μ_8 bridges.

In Ag_2Se the Ag atoms have trigonal and tetrahedral coordination. In agreement with this, the Ag atoms in **3** and **4** are also coordinated by Se atoms in trigonal and tetrahedral environments. There are 14 P*t*Bu$_3$ ligands (P1–P7) bound to the cluster surface of **3**, and four dppp ligands to the surface of **4**. The silver atoms bound to these P atoms have distorted tetrahedral coordination.

With increasing cluster size, the distribution of the Ag atoms in the molecular structure becomes more chaotic. As a result, problems emerged in the refinement of **4**. However, this shows that one can assume that in compounds **1**–**4** one has in reality ligand-protected sections of the Ag_2Se structure, because in the solid bulk material of Ag_2Se the Ag^+ anions are disordered.[9] This is probably also the reason for the fact that in the analogous reaction to Equation (3) of silver acetate, P*t*Bu$_3$, and *n*BuSeSiMe$_3$, cluster **5** is formed [Eq. (4)]. The structure of

$$CH_3CO_2Ag \xrightarrow[PtBu_3]{nBuSeSiMe_3} [Ag_{112}Se_{32}(SenBu)_{48}(PtBu_3)_{12}] \quad \mathbf{5} \qquad (4)$$

5 is almost identical to that of **3**. The difference to **3** lies in the number of phosphane ligands coordinated to the cluster surface; this is why **5** has two Ag atoms less than **3**. The number of Se atoms and their structure are identical in **3** and **5**; however, the ratio of Se^{2-} to Se*n*Bu$^-$ ligands is different.

The silver clusters **1**–**5** are formed in part from breaking the Se–C bond in *t*BuSeSiMe$_3$ and *n*BuSeSiMe$_3$. As a result of a redox reaction complexes are produced with Se^{2-} and SeR^- ligands, whose cluster surface is covered with phosphane ligands and the organic groups bound to selenium. The influence of the phosphane ligands on the structure of the silver–selenium core is made clearer, in that they evidently are able to intervene in the formation of stable Ag_2Se and AgSeR at specific steps. However, it is still unclear why this should lead to the formation of defined structures that are reproducible under the given experimental conditions. It may be possible that this is determined by the surface energy of the cluster molecule. Calculations for this are currently being carried out. On the assumption that in **1**–**5** Se^{2-} and SeR^- ligands exist, all the Ag atoms must possess a formal charge of

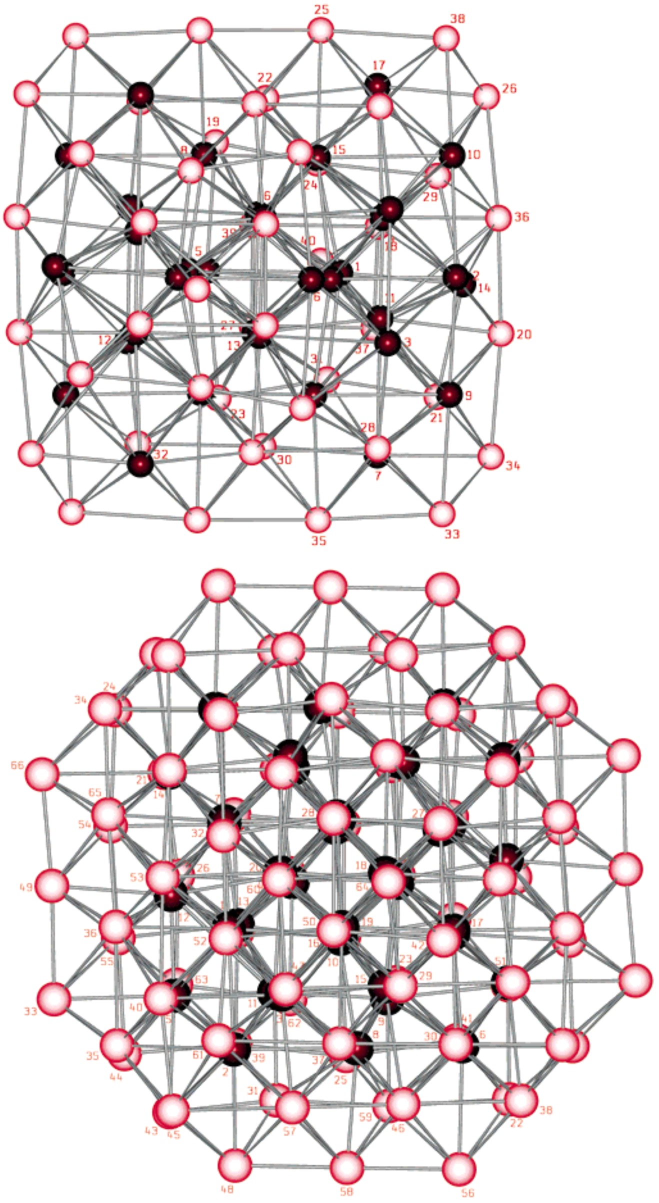

Figure 5. Skeleton structure of the Se atoms in **3** (above) and **4** (below). The Se^{2-} ligands are shown in dark red, and the Se atoms from the Se*n*Bu groups in light red.

1 + (d^{10} configuration). Correspondingly there is no evidence of Ag−Ag interactions; all Ag−Ag distances are greater than 290 pm.

Experimental Section

1: P*n*Pr_3 (0.26 mL, 1.31 mmol) was added to a solution pf$PhCO_2Ag$ (0.15 g, 0.65 mmol) in pentane (10 mL) at −40°C. Then *t*BuSeSiMe_3 (0.20 mL, 0.86 mmol) was added. After a short time a clear solution was formed. Within 2 d the solution turned dark green from which orange crystals of **1** were formed (yield: 60%).

2: In an analogous way to **1** $PhCO_2Ag$ (0.15 g, 0.65 mmol) in THF (10 mL) was treated at −40°C with PEt_3 (0.10 mL, 0.64 mmol) and *t*BuSeSiMe_3 (0.20 mL, 0.86 mmol). After a few minutes a dark brown solution was formed. After a further 2 d black platelets of **2** crystallized (yield: 60%).

3: $C_{11}H_{23}CO_2Ag$ (0.10 g, 0.33 mmol) in pentane (10 mL) was treated with P*t*Bu_3 (0.30 mL, 1.26 mmol) and *n*BuSeSiMe_3 (0.10 mL, 0.43 mmol) at −30°C. Black crystals of **3** were formed after about 14 d from the deeply colored solution (yield: 30%).

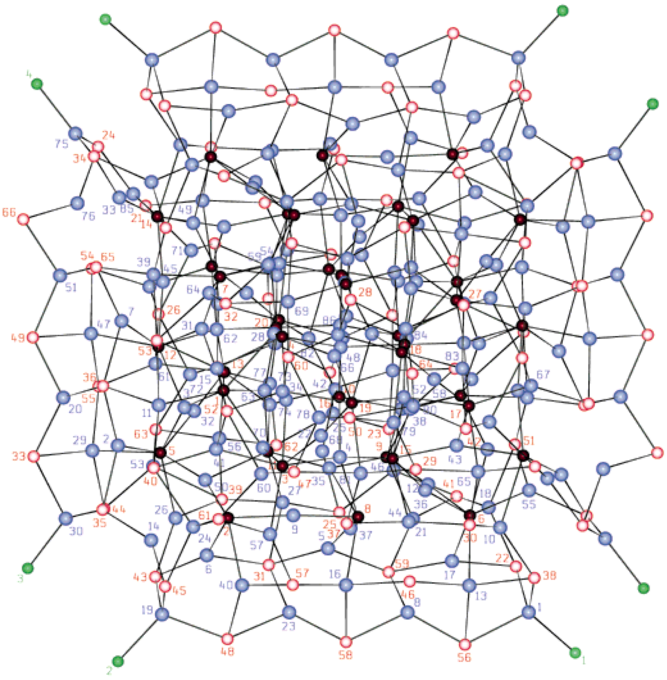

Figure 6. Molecular structure of **4** (without C atoms).[12] The P atoms are colored green, Se^{2-} ligands red, Se atoms from the Se*n*Bu-ligands light red, and Ag atoms blue. The atom number is given and the corresponding atom type can be deduced from the color. Selected bond lengths (±0.7 pm) and angles (±0.2°): Ag9−Se2 254.4(6), Ag9−Se8 255.0(6), Ag2−Se5 272.6, Ag2−Se5 2585, Ag2−Se36 257.2, Ag4−Se3 279.9, Ag4−Se8 278.1, Ag4−Se15 278.4, Ag4−Se16 267.1; Se2-Ag9-Se8 176.2, Se5-Ag2-Se35 92.3, Se5-Ag2-Se36 121.9, Se35-Ag2-Se36 145.3, Se3-Ag4-Se8 112.6, Se3-Ag4-Se15 101.1, Se3-Ag4-Se16 112.4, Se8-Ag4-Se15 97.2, Se8-Ag4-Se16 120.4, Se15-Ag4-Se16 110.2.

4: $C_{11}H_{23}CO_2Ag$ (0.32 g, 1.04 mmol) in CHCl3/toluene (1/3, 10 mL) was treated with dppp (0.11 g, 0.26 mmol) and *n*BuSeSiMe_3 (0.25 mL, 0.05 mmol) at −20°C. After 2 d reaction time the solution was allowed to slowly warm up to room temperature. Within 14 d black crystals of **4** were formed from the dark brown solution together with Ag_2Se (yield: 20%)

5: AgAc (0.10 g, 0.60 mmol) in pentane/THF (1/1, 10 mL) was treated with P*t*Bu_3 (0.25 mL, 1.05 mmol) and P*n*Bu_3 (0.20 mL, 0.86 mmol) at −30°C. After 28 d black crystals of **5** were formed (yield: 60%).

The results of the elemental analyses of **1**–**5** (Ag, P, Se) agree with the given empirical formulae.

Received: May 15, 1998 [Z11863IE]
German version: *Angew. Chem.* **1998**, *110*, 2783–2788

Keywords: clusters · selenium · silver · structure elucidation

---

[1] *Clusters and Colloids. From Theory to Applications* (Ed.: G. Schmid), VCH, Weinheim, **1994**; *Physics and Chemistry of Metal Cluster Compounds* (Ed.: L. J. de Jongh), Kluwer, Dordrecht, **1994**.

[2] I. Dance, K. Fisher, *Prog. Inorg. Chem.* **1994**, *41*, 637; L. C. Roof, J. W. Kolis, *Chem. Rev.* **1993**, *93*, 1037; J. Arnold, *Prog. Inorg. Chem.* **1995**, *43*, 353.

[3] D. Ohlmann, H. Pritzkow, H. Grützmacher, M. Anthamatten, R. Glaser, *J. Chem. Soc. Chem. Commun.* **1995**, 1011; B. J. Bonasis, G. P. Mitchell, F. J. Hollander, J. Arnold, *Inorg. Chem.* **1994**, *33*, 1797; J. Zhao, D. Adcock, W. T. Pennington, J. W. Kolis, *Inorg. Chem.* **1990**, *29*, 4358; I. Dance, G. Lee, *Spec. Publ. R. Soc. Chem.* **1993**, 131; J. G. Brennan, T. Siegrist, P. J. Carrol, S. H. Stuczynski, P. Reynders, L. E. Brus, M. L. Steigerwald, *Chem. Mater.* **1990**, *2*, 403.

[4] D. Fenske, J. Ohmer, J. Hachgenei, *Angew. Chem.* **1985**, *97*, 993; *Angew. Chem. Int. Ed. Engl.* **1985**, *24*, 993; D. Fenske, J. Ohmer, J.

Hachgenei, K. Merzweiler, *Angew. Chem.* **1988**, *100*, 1300; *Angew. Chem. Int. Ed. Engl.* **1988**, *27*, 1277.

[5] H. Krautscheid, D. Fenske, G. Baum, M. Semmelmann, *Angew. Chem.* **1993**, *105*, 1364; *Angew. Chem. Int. Ed. Engl.* **1993**, *32*, 1303.

[6] D. Fenske, H. Krautscheid, *Angew. Chem.* **1990**, *102*, 799; *Angew. Chem. Int. Ed. Engl.* **1990**, *29*, 796.

[7] S. Dehnen, A. Schäfer, R. Ahlrichs, D. Fenske, *Chem. Eur. J.* **1996**, *2*, 429; S. Dehnen, A. Schäfer, D. Fenske, R. Ahlrichs, Angew. *Chem.* **1994**, *106*, 786; *Angew. Chem. Int. Ed. Engl.* **1994**, *33*, 746.

[8] D. van der Putten, D. Olevano, R. Zanoni, H. Krautscheid, D. Fenske, *J. Electron Spectrosc.* **1995**, *76*, 207.

[9] J. F. Corrigan, D. Fenske, *Chem. Commun.* **1996**, 943; J. F. Corrigan, D. Fenske, *Chem. Commun.* **1997**, 1837; J. F. Corrigan, D. Fenske, W. P. Power, *Angew. Chem.* **1997**, *109*, 1224; *Angew. Chem. Int. Ed. Engl.* **1997**, *36*, 1176.

[10] G. A. Wiegers, *Am. Mineral.* **1971**, *56*, 1882; Z. G. Pinsker, C. Chiang-liang, R. M. Imamov, E. L. Lapidus, *Sov. Phys. Crystallogr. (Engl. Transl.)* **1965**, *7*, 225.

[11] S. Dehnen, D. Fenske, *Angew. Chem.* **1994**, *106*, 2369; *Angew. Chem. Int. Ed. Engl.* **1994**, *33*, 2287; S. Dehnen, D. Fenske, *Chem. Eur. J.* **1996**, *2*, 1407; S. Dehnen, D. Fenske, A. C. Deveson, *J. Cluster Sci.* **1996**, *3*, 351; A. C. Deveson, S. Dehnen, D. Fenske, *J. Chem. Soc. Dalton Trans.* **1997**, 4491.

[12] Crystal structure analysis: STOE-IPDS ($Mo_{K\alpha}$ radiation); Data collection and refinement (SHELXS-86, SHELXL-93); empirical corrections (habit). **1**: triclinic, space group $P\bar{1}$ (no. 2), $Z=1$, lattice constants (190 K): $a=1770.4(4)$, $b=1849.1(4)$, $c=1856.1(4)$ pm, $\alpha=96.21(3)$, $\beta=101.49(3)$, $\gamma=93.34(3)^\circ$, $V=5900\times10^6$ pm^3, $\mu(Mo_{K\alpha})=5.901$ mm^{-1}, $2\Theta_{max.}=50^\circ$; of 22182 reflections measured, 16085 were independent ($R_{int}=0.082$) and 11914 observed with $I>2\sigma(I)$; 667 parameters (Ag, Se, P, anisotropic and C isotropic); max. residual electron density: 2.7 e Å^3; $R_1=0.070$; $wR_2=0.18$. **2**: triclinic, space group $P\bar{1}$ (no. 2), $Z=1$, lattice constants (170 K): $a=2025.0(4)$, $b=2521.2(5)$ $c=2643.1(5)$ pm, $\alpha=61.15(2)$, $\beta=80.10(3)$, $\gamma=67.36(3)^\circ$, $V=11629\times10^6$ pm^3, $\mu(Mo_{K\alpha})=7.85$ mm^{-1}, $2\Theta_{max.}=52^\circ$; of 64995 reflections measured, 41759 were independent ($R_{int}=0.10$) and 21790 observed with $I>2\sigma(I)$; 1110 parameters (Ag, Se, P, anisotropic, C isotropic); max. residual electron density 2.8 e Å^{-3}; $R_1=0.098$; $wR_2=0.28$. **3**: triclinic, space group $P\bar{1}$ (no. 2), $Z=1$, lattice constants (170 K): $a=2619.4(5)$, $b=2765.9(6)$ $c=2815.7(6)$ pm, $\alpha=116.39(3)$, $\beta=91.46(3)$, $\gamma=100.30(3)^\circ$, $V=17851.0\times10^6$ pm^3, $\mu(Mo_{K\alpha})=7.18$ mm^{-1}, $2\Theta_{max.}=50^\circ$; of 56227 reflections measured, 43345 were independent ($R_{int}=0.10$) and 20294 observed with $I>2\sigma(I)$; 1330 parameters (Ag, Se anisotropic, P, C isotropic); max. residual electron density 2.7 e Å^{-3}; $R_1=0.089$; $wR_2=0.22$. **4**: triclinic, space group $P\bar{1}$ (no. 2), $Z=1$, lattice constants (170 K): $a=2824.0(6)$, $b=2980.0(6)$ $c=3225.0(6)$ pm, $\alpha=67.14(3)$, $\beta=68.02(3)$, $\gamma=67.94(3)^\circ$, $V=22333\times10^6$ pm^3, $\mu(Mo_{K\alpha})=9.09$ mm^{-1}, $2\Theta_{max.}=48^\circ$; of 99240 reflections measured, 64156 were independent and 22753 observed with $I>2\sigma(I)$; 1933 parameters (Ag, Se, P, anisotropic, C isotropic); max. residual electron density 4.8 e Å^{-3}; $R_1=0.12$; $wR_2=0.35$. The high R value is partly a result of the fact that a portion of the C atoms on the *n*Bu groups could not be localized. Apart from that it was not possible to distinguish the disordered solvent molecules. **5**: **5**·2THF; triclinic, space group $P\bar{1}$ (no. 2), $Z=1$, lattice constants (170 K): $a=2598.3(5)$, $b=2626.1(8)$ $c=2952.9(6)$ pm, $\alpha=112.85(3)$, $\beta=112.11(3)$, $\gamma=90.61(3)^\circ$, $V=16911\times10^6$ pm^3, $\mu(Mo_{K\alpha})=7.52$ mm^{-1}, $2\Theta_{max.}=50^\circ$; of 70408 relections measured, 49109 were independent and 35916 observed with $I>2\sigma(I)$; 1623 parameters (Ag, Se, P, anisotropic, C isotropic); max. residual electron density 3.1 e Å^{-3}; $R_1=0.065$; $wR_2=0.18$. Further details on the crystal structure investigation may be obtained from the Fachinformationszentrum Karlsruhe, D-76344 Eggenstein-Leopoldshafen, Germany (fax: (+49)7247-808-666; e-mail: crysdata@fiz-karlsruhe.de), on quoting the depository numbers CSD-408688 to CSD-408692.

[13] K. Eichkorn, U. Schneider, R. Ahlrichs, *J. Chem. Phys.* **102**, *19*, 7557; C. Ochsenfeld, R. Ahlrichs, *Ber. Bunsen-Ges. Phys. Chem.* **1994**, *98*, 34; C. Ochsenfeld, J. Gauss, R. Ahlrichs, *J. Chem. Phys.* **1995**, *103*, 7401; C. Ochsenfeld, R. Ahlrichs, *J. Chem. Phys.* **1994**, *101*, 5977; C. Ochsenfeld, R. Ahlrichs, *Ber. Bunsen-Ges. Phys. Chem.* **1995**, *99*, 1191.

[14] I. G. Dance, K. J. Fisher, *J. Chem. Soc. Dalton Trans.* **1997**, 2563.

Detection of Catalytic Activity in Combinatorial Libraries of Heterogeneous Catalysts by IR Thermography

Arnold Holzwarth, Hans-Werner Schmidt, and Wilhelm F. Maier*

The ever increasing need for more selective heterogeneous catalysts in chemical processing cannot be satisfied by conventional catalyst development and, therefore, combinatorial approaches should be considered. The combinatorial synthesis and screening of large numbers of organic compounds is already an established tool for the development of new pharmaceuticals,[1] while the combinatorial approach to the development of new solid materials has just started. In 1995 the first combinatorial developments of new materials, like new magnetoresists[2] and new superconductors[3] were reported. In 1997 libraries produced efficiently by wet-chemical syntheses with the help of ink-jet technology were created for the development of new luminescent materials.[4] New blue photoluminescent materials followed in 1998.[5] The true potential of the combinatorial approach to materials development becomes apparent by reports on thin film libraries of 25000 different materials on 7.5-cm diameter substrates. These libraries were prepared by thin film technologies using physical evaporation techniques.[6] To apply such techniques to the development of new heterogeneous catalyst materials an efficient method for the reliable spatially resolved detection of catalytic activities is required. Promising recent developments are the use of spatially resolved ionization techniques.[7] In the above-mentioned development of photoluminescent materials charge-coupled detector (CCD) cameras were applied which have excellent spatial resolution.[4–6] For the simultaneous display of catalytic activities on a catalyst library an IR-video camera appears attractive.

The applicability of IR thermography in heterogeneous catalysis was demonstrated already in 1987, where oscillations in a catalytic reaction of hydrogen with oxygen across a 4 cm^2 catalyst wafer could be monitored.[8a] Since this is a very exothermic reaction (241 kJ mol^{-1}), the temperature variations were as large as 70 °C. In the same year temperature differences smaller than 5 °C were measured for the hydrogenation of cyclohexene on Pt/SiO_2 catalysts with IR thermography.[8b] This technique was later applied to the screening of heterogeneous catalysts for hydrogen oxidation on 16 free-standing catalyst pellets.[9] Since the size of the catalyst pellets (4 × 3 mm) and the temperature differences observed (80 °C) limit both the spatial and the thermal resolution of these experiments, there is little prospect for application of such thermographic methods for the reliable detection of catalytic activity on large catalyst libraries with its microscopic amounts of catalysts. More promising is a recent report on the application of IR-thermographic methods for the combinatorial selection of small encoded polymer bead catalysts in

---

[*] Prof. Dr. W. F. Maier, Dr. A. Holzwarth, H.-W. Schmidt
Max-Planck-Institut für Kohlenforschung
Kaiser-Wilhelm-Platz 1, D-45470 Mülheim an der Ruhr (Germany)
Fax: (+49) 208-306-2987
E-mail: maier@mpi-muelheim.mpg.de